JOURNAL OF AIRCRAFT
Vol. 44, No. 1, January–February 2007

Effect of Microvortex Generators on Separated Normal Shock/Boundary Layer Interactions

H. Holden* and H. Babinsky†
Cambridge University, Cambridge, CB2 1PZ, United Kingdom

DOI: 10.2514/1.22770

Experiments have been performed in a blowdown supersonic wind tunnel to investigate the effect of subboundary layer vortex generators placed upstream of a normal shock/turbulent boundary layer interaction at a Mach number of 1.5 and a freestream Reynolds number of 28×10^6. The Reynolds number based on the inflow boundary layer displacement thickness was 26,000. Two types of subboundary layer vortex generators were investigated: wedge-shaped and counter-rotating vanes. It was found that the vane-type subboundary layer vortex generators eliminated and the wedge-type subboundary layer vortex generators greatly reduced the shock-induced separation. When placed in the supersonic part of the flow, both types of subboundary layer vortex generators caused a wave pattern consisting of a shock, reexpansion, and shock. The reexpansion and double shocks are undesirable features because they equate to increased total pressure losses. Furthermore there are indications that the vortex intensity is reduced by the normal shock/boundary layer interaction. Overall, the vane-type subboundary layer vortex generators were the more effective devices as they eliminated the shock-induced separation and had the least detrimental effect on the shock structure.

Nomenclature

H_i	=	shape factor $=\delta^*/\theta$
h	=	vortex generator height
M	=	Mach number
P	=	pressure
R	=	reattachment
S	=	separation
U	=	freestream flow velocity, ms^{-1}
u	=	local flow velocity, ms^{-1}
X	=	streamwise coordinate, mm
Y	=	vertical coordinate, mm
Z	=	spanwise coordinate, mm
δ	=	boundary layer thickness, mm
δ^*	=	boundary layer displacement thickness, mm $= \int_0^\delta (1 - \rho u/\rho_e U_e)\,\mathrm{d}y$
θ	=	boundary layer momentum thickness, mm $= \int_0^\delta \rho u/\rho_e U_e (1 - \rho u/\rho_e U_e)\,\mathrm{d}y$

Subscripts

0	=	total conditions
1	=	upstream of shock
∞	=	freestream

Introduction

VORTEX generators (VGs) are widely used in aviation applications, for instance in the intakes to supersonic jet engines and on the wings of civil aircraft. Their purpose is to control boundary layer separation due to adverse pressure gradients [1,2] and shock-induced separation [2,3]. They have also been used to reduce fluctuating pressure loads for buffet control [4,5]. VGs energize the boundary layer by enhancing mixing between the higher momentum external flow and the low momentum near-wall flow. However, there is an obvious disadvantage in using VGs because they cause a parasitic drag component [6]. More recent work has found that subboundary layer vortex generators (SBVGs), see Fig. 1, which carry a much lower drag penalty, can be effective at flow separation control [1,7,8].

Ashill et al. [8] investigated SBVGs on an airfoil model at low speed and in transonic flow. They showed that at transonic speeds the SBVGs delayed the onset of flow separation at the trailing edge, with the *vane-type SBVGs* being the most effective; these results were consistent with the low-speed studies. They also found that one of the SBVGs investigated, a wedge shape, seemed to reduce the shock strength on transonic airfoils. Ashill et al. suggest that this could be due to the SBVG generating compression waves that weaken the main shock wave. This observation is of interest because it ties in with shock-control methods such as passive devices [2,9–11], active control [2] using blowing [2] or suction [12,13], and 2-D [14,15] or 3-D bumps [16], which work by generating compression waves that smear the shock-induced pressure rise. However, Inger and Siebersma [17] showed numerically that VGs upstream of a shock energize the boundary layer, thereby reducing the shape factor and increasing the pressure gradient and shock strength across the interaction. This paper presents an investigation into the effect of SBVGs upstream of a separated shock/boundary layer interaction (SBLI) and aims to determine whether such devices can have a shock weakening effect. The SBVGs investigated were based on those used by Ashill et al.

Experimental Arrangement

The experimental investigation was performed in a blowdown supersonic wind tunnel at the University of Cambridge (a typical run time of 45 s). Figure 2a shows the tunnel arrangement and control region. Shaped liners in the upstream throat gave uniform parallel flow with a nominal Mach number of 1.5 ahead of the shock. The stagnation pressure and temperature are 1.8×10^5 Pa and 292 K, respectively. The working section is 114 mm wide, 172 mm long, and 178 mm tall. Manual adjustment of the freestream stagnation pressure and second throat allows a recovery shock to be held at a given location in the parallel part of the working section. Three shock positions were investigated, the same as those used for other flow control studies in the wind tunnel [11,16,18]. The second and third shock positions exhibited very similar behavior, and so this discussion concentrates on the first two shock positions (hereafter

Received 27 January 2006; accepted for publication 21 April 2006. Copyright © 2006 by H. A. Holden and H. Babinsky. Published by the American Institute of Aeronautics and Astronautics, Inc., with permission. Copies of this paper may be made for personal or internal use, on condition that the copier pay the $10.00 per-copy fee to the Copyright Clearance Center, Inc., 222 Rosewood Drive, Danvers, MA 01923; include the code $10.00 in correspondence with the CCC.

*Engineering Department, Trumpington Street. AIAA member.
†Reader in Aerodynamics, Engineering Department, Trumpington Street. AIAA member.

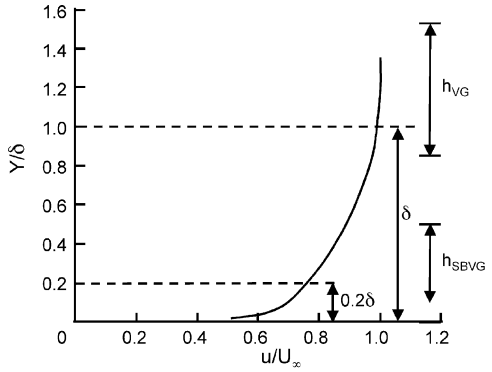

Fig. 1 SBVG height relative to the turbulent boundary layer velocity profile [1].

termed "front" and "middle," which are at $X = -36$ mm and $X = 0$ mm relative to the center of the working section). The experiments made use of the interaction between the shock wave and the naturally grown turbulent boundary layer on the tunnel floor. The incoming boundary layer (at $X = -30$ mm) is approximately 5.7 mm thick and $\delta^* = 1.02$ mm. The Reynolds number based on boundary layer displacement thickness is approximately 26,000.

Two types of SBVGs were investigated, *vane-type SBVGs* and *wedge-type SBVGs*, based on those investigated by Ashill et. al. [8]. The vane-type SBVGs (Fig. 2b) were supplied by QinetiQ (formerly DERA Bedford) and were used in the study by Ashill et al. [8]. The vane-type SBVGs have a height of 1.25 mm, which gave a ratio of $h/\delta^* = 1.3$ (as opposed to $h/\delta^* = 1.6$ when they were used by Ashill et. al), and were placed 15 mm($\simeq 12h$) apart, as was done in the earlier investigation. The wedge-type SBVGs (Fig. 2c) were constructed for the current experiments; they are 2 mm tall (giving a ratio of $h/\delta^* = 2.13$) and were spaced 18 mm apart. Both types of SBVG were arrayed symmetrically about the tunnel centerline, with their leading edges at $X = -50$ mm.

Surface pressure measurements were made using Druck PDCR-200 miniature pressure transducers connected to the pressure tappings shown in Fig. 2d. Boundary layer traverses were performed downstream of the interaction using a flat-headed pitot probe (dimensions 1.61×0.131 mm) connected to a pressure transducer. Surface oil-flow visualization was performed using a paraffin, titanium dioxide, and oleic acid mixture.

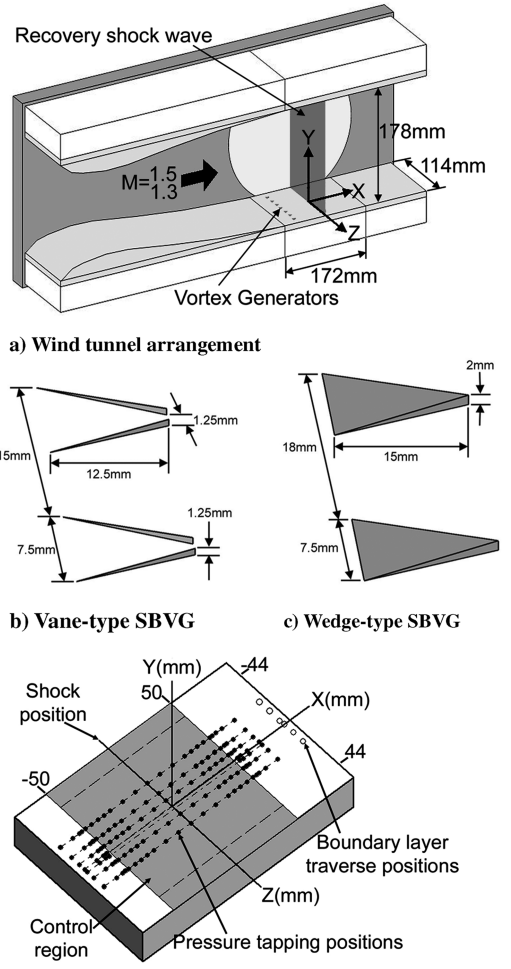

Fig. 2 Experimental arrangement.

Experimental Accuracy

The experimental error in the surface static and pitot pressures is on the order of $\pm 1\%$. The traverse gear used to measure boundary layer profiles had an accuracy better than 0.1 mm (0.5% of the boundary layer thickness). A degree of unsteadiness was observed in the shock wave, resulting in an error in streamwise location on the order of 3 mm.

Results

Uncontrolled Interaction

Figure 3 shows, from left to right, a schlieren photograph, wall pressure measurements, and surface oil-flow visualization for the uncontrolled interaction. The schlieren picture indicates that the flow has separated; there is a small λ structure where the shock foot interacts with the boundary layer. A faint slipline can be seen extending downstream from the triple point. Slight imperfections in the tunnel wall cause a spurious wave to emanate from upstream of the interaction. There are also a number of weak waves caused by pressure tapping points on the surface. None of these have a significant effect on the flow, which is confirmed by the nearly constant value of the wall pressure measurements before the shock. There is no plateau in the wall pressure measurements at the λ shock location because the length of the separated region is still quite short and there is insufficient data in this region. The surface oil-flow visualization does show a distinct separation line (unfortunately slightly smeared during tunnel shutdown) and a region where reattachment probably occurs. The position of the separation line agrees well with the location of the λ shock leading leg in the schlieren picture; the reattachment region occurs slightly after the rear leg. The separation line is approximately normal to the freestream direction and fairly 2-D in the center of the tunnel, but

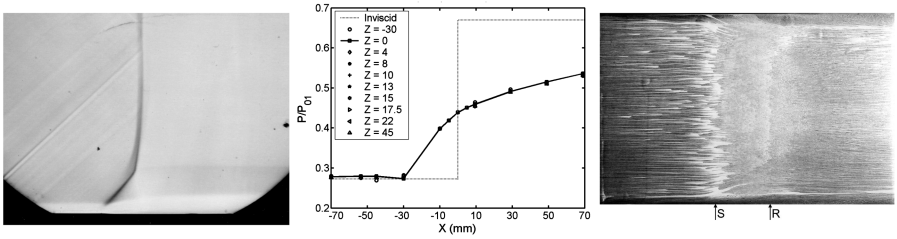

Fig. 3 No control schlieren picture, wall pressure measurements, and surface oil-flow visualization.

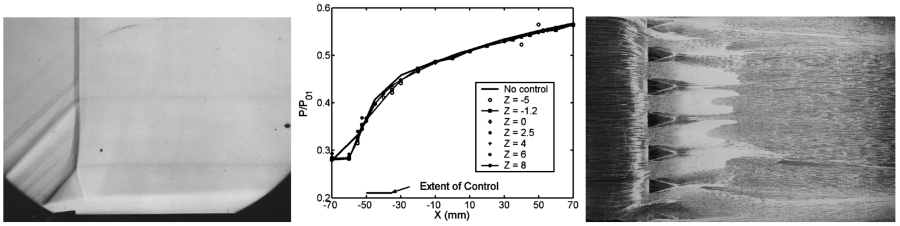

a) Shock front

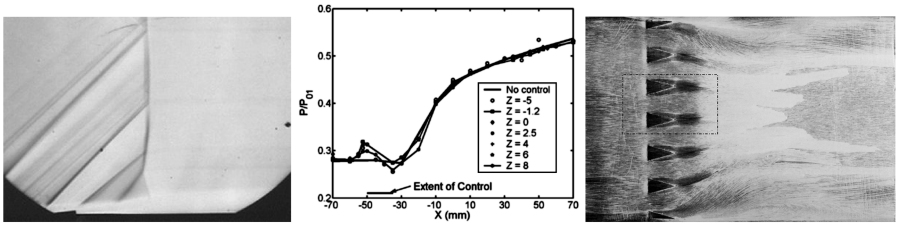

b) Shock middle

Fig. 4 Wedge-type SBVG schlieren pictures, wall pressure measurements, and surface oil-flow visualizations.

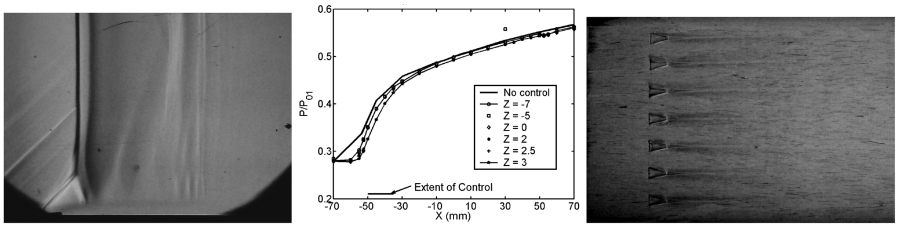

a) Shock front

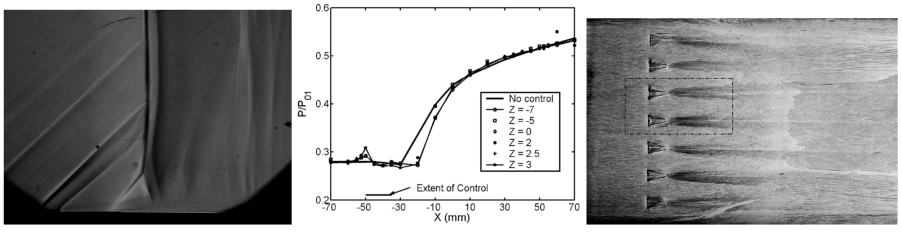

b) Shock middle

Fig. 5 Vane-type SBVG schlieren pictures, wall pressure measurements, and surface oil-flow visualizations.

there is curvature at the edges due to the interaction with the sidewall boundary layers. The separations at the tunnel sidewalls occupy approximately 8% of the tunnel span at the middle shock position, $X = 0$ mm. The incoming boundary layer at $X = -30$ mm is approximately 5.7 mm thick ($\delta^* = 1.02$ mm, $\theta = 0.67$ mm, and $H = 1.51$). After the shock the boundary layer has doubled in thickness to about 12.2 mm, and it is much less full at $X = 50$ mm, $\delta^* = 5.06$ mm, $\theta = 1.82$ mm, and $H = 2.78$.

Subboundary Layer Vortex Generators

Figures 4 and 5 depict the flow structure with the wedge-type and vane-type SBVGs located upstream of the shock wave. When the main shock is in the front position, close to the SBVG trailing edges (Figs. 4a and 5a), the schlieren pictures resemble the uncontrolled interaction. When the shock is in the middle position (Figs. 4b and 5b), there is a leading shock at the start of each SBVG followed by a reexpansion and a second shock at its trailing edge. Downstream of the SBVGs the main shock resembles that seen in the uncontrolled interaction, except that the λ foot is distinctly smaller. This contraction of the λ foot appears to confirm the conclusions of Inger and Siebersma [17] that VGs reduce the size of the interaction region. The boundary layer thickens significantly at the main shock position for both devices.

The wall pressure measurements reflect the behavior seen in the schlieren pictures. In the front shock position the SBVGs have little effect on the strength of the shock-induced pressure rise. In the middle shock position the wall pressure measurements show a shock-

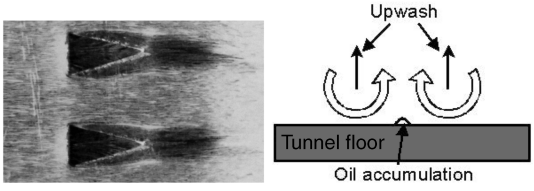

a) Wedge-type SBVG

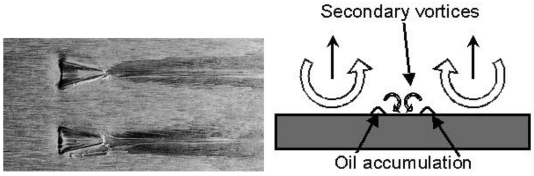

b) Vane-type SBVG

Fig. 6 SBVGs, shock middle, surface oil-flow visualization details and diagrams of proposed vortex structure.

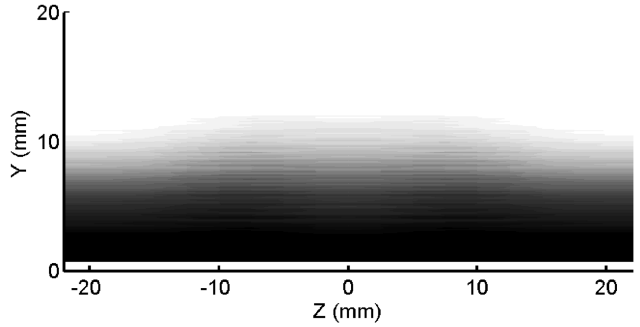

a) No control

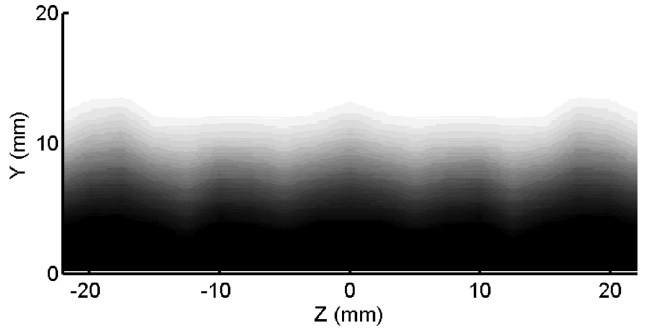

b) Wedge-type SBVG

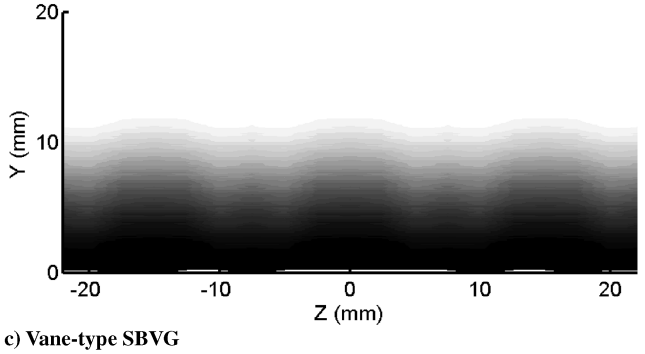

c) Vane-type SBVG

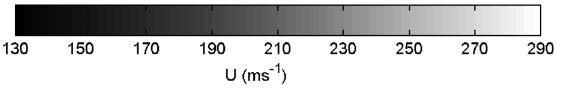

d) Scale

Fig. 7 No control and SBVGs velocity maps, shock middle, $X = 90$ mm.

reexpansion-shock structure over the SBVG followed by a main shock that is at least as strong as in the uncontrolled interaction. The SBVGs cause a fairly 3-D shock structure at both shock positions. This is clearest in the wall pressure measurements for the middle shock position (for example, see Fig. 4b) where the leading shock is most pronounced closest to the device centerline, reducing in severity with increasing spanwise distance. The Mach number ahead of the main shock is likely to be as high (or higher) as that seen in the uncontrolled interaction because of the reexpansion over the SBVGs and the associated flow acceleration. The total pressure losses (and hence wave drag) caused by the SBVGs are therefore likely to be greater than for the uncontrolled interaction. Of the two types of SBVG the vane-type SBVGs cause a weaker reexpansion and will therefore have a less detrimental effect on the total pressure losses.

Figure 4 shows the surface oil-flow visualization for the wedge-type SBVGs. There is a dark region of high shear flow downstream of the devices, which disappears at the main shock position, suggesting that the shock has a "damping" effect on the vortices. There is then a large region of oil-flow deposition (this was unfortunately smeared during tunnel shutdown), which suggests that the flow velocities are slow here. Comparison with the surface oil-flow visualization for the uncontrolled interaction (Fig. 3) shows that the sidewall separation is more extensive when the wedge-type SBVGs are in the tunnel. The wedge-type SBVGs appear to reduce the size of the shock-induced separation, but not eliminate it. The surface oil-flow visualization for the vane-type SBVGs suggests that they eliminate the shock-induced separation entirely (Fig. 5). The footprints of the vortices produced by the vane-type SBVGs can still be seen very clearly several incoming boundary layer thicknesses downstream of the shock position, whereas they cannot for the wedge-type SBVGs. This suggests that the vane-type SBVGs cause either stronger vortices or vortices that lift off the surface more slowly.

Figure 6a depicts a detail of the surface oil-flow visualization over the wedge-type SBVG and the probable vortex structure. The flow over the vane-type SBVGs is more complex (Fig. 6b); within the dark region of high shear flow downstream of each device pair there are two distinct white lines where oil flow has been deposited. These are probably separation lines, occurring because the devices produce two pairs of counter-rotating vortices as sketched in the diagram. The more widely spaced primary vortices produced by the vane-type SBVGs are likely to produce less upwash and so lift off the surface more slowly than those caused by the wedge-type SBVGs.

Figure 7 compares the streamwise boundary layer velocity profiles at $X = 90$ mm. The SBVGs produce a slightly thicker boundary layer than the uncontrolled interaction, with distinct spanwise variations in the boundary layer thickness, which is more pronounced for the vane-type SBVGs. Figure 8 makes it easier to determine the presence of the vortices by removing the effect of the boundary layer. This was achieved by subtracting the velocities measured with control (Figs. 7b and 7c) from that without control (Fig. 7a). In the resulting image the difference in velocities due to the presence of the vortices can be seen more clearly. Of the two types of

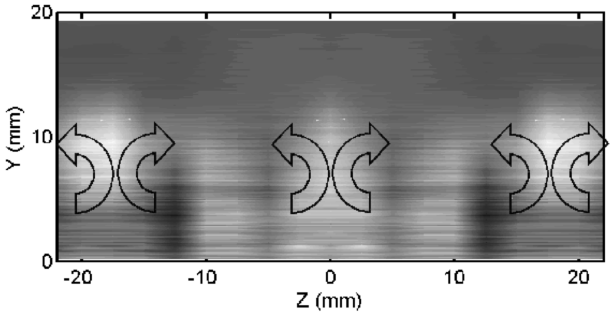

a) Wedge-type SBVG

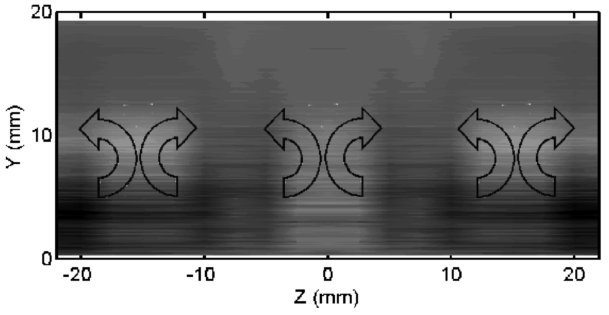

b) Vane-type SBVG

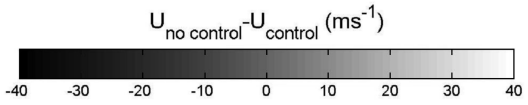

c) Scale

Fig. 8 SBVGs velocity deficit, shock middle, $X = 90$ mm.

SBVGs the vane-type SBVGs produce, on average, higher velocities, especially close to the surface. The wedge-type SBVGs produce much lower velocities, especially in the vortex core. This might explain why the vane-type SBVGs are more successful at preventing the shock-induced separation by energizing the boundary layer.

Conclusions

SBVGs placed upstream of a separated SBLI have been investigated to study their effects on wave drag and the separation. When the shock is located directly over the SBVGs, the SBLI resembles that seen in the uncontrolled interaction. However, when the shock is downstream of the SBVGs, a shock-reexpansion-shock structure develops over the devices followed by the main shock. This means that, except when the main shock is directly over the devices, SBVGs upstream of the shock cause increased wave drag. Of the two types of SBVG investigated, the vane-type SBVGs had the least detrimental effect on the shock structure.

For both types of SBVG the high shear region observed in the surface oil-flow visualization disappeared at the shock location; it appears that the shock has a "damping" effect on the vortices. The vane-type SBVGs are the more effective devices because they were observed to eliminate a shock-induced separation. This appears to be because they produce vortices that are slightly farther apart and more energetic, thus lifting off the surface more slowly and energizing the boundary layer more effectively. The fact that SBVGs have been successful in eliminating a shock-induced separation is an important result because the drag penalty associated with SBVGs is much less than for conventional vortex generators.

Acknowledgements

The authors are grateful for the financial support of the Engineering and Physical Sciences Research Council (EPSRC) United Kingdom, GKN Westland, and Thales Underwater Systems and to Clyde Warsop at BAE Systems for his continuing interest and support. The authors are indebted to the technicians at the Aeronautical Laboratory, Department of Engineering, University of Cambridge, for their expert model making and for tirelessly running the wind tunnel. The authors would like to thank QinetiQ (formerly DERA Bedford) for supplying the vane-type SBVGs.

References

[1] Lin, J. C., "Review of Research on Low-Profile Vortex Generators to Control Boundary-Layer Separation," *Progress in Aerospace Sciences*, Vol. 38, No. 4–5, May–July 2002, pp. 389–420.

[2] Delery, J., "Shock Wave/Turbulent Boundary Layer Interaction and its Control," *Progress in Aerospace Sciences*, Vol. 22, No. 4, 1985, pp. 209–280.

[3] Pearcey, H., "Boundary Layer Control for Aerofoils and Wings," *Boundary Layer and Flow Control: Its Principles and Application*, Vol. 2, edited by G. Lachmann, Pergamon Press, Oxford, 1961, Chap. 4, pp. 1261–1333.

[4] Barter, J. W., and Dolling, D. S., "Reduction of Fluctuating Pressure Loads in Shock/Boundary-Layer Interactions," *AIAA Journal*, Vol. 33, No. 10, 1995, pp. 1842–1849.

[5] Bean, D., Greenwell, D., and Wood, N., "Vortex Control Technique for the Attenuation of Fin Buffet," *Journal of Aircraft*, Vol. 30, No. 6, Nov.–Dec. 1993, pp. 847–853.

[6] Kusunose, K., and Yu, N., "Vortex Generator Installation Drag on an Airplane Near Its Cruise Condition," AIAA Paper 03-0932, Jan. 2003.

[7] Wendt, B., and Hingst, W., "Flow Structures in the Wake of a Wishbone Vortex Generator," *AIAA Journal*, Vol. 32, No. 11, Nov. 1994, pp. 2234–2240.

[8] Ashill, P., Fulker, J., and Hackett, K., "Research at DERA on Sub-Boundary Layer Vortex Generators (SBVGs)," AIAA Paper 01-0831, Jan. 2001.

[9] Chokani, N., and Squire, L., "Transonic Shockwave/Turbulent Boundary Layer Interactions on a Porous Surface," *Aeronautical Journal*, Vol. 97, No. 965, May 1993, pp. 163–170.

[10] Gibson, T., Babinsky, H., and Squire, L., "Passive Control of Shock Wave—Boundary-Layer Interactions," *Aeronautical Journal*, Vol. 104, No. 1033, 2000, pp. 129–140.

[11] Smith, A., Babinsky, H., Fulker, J., and Ashill, P., "Normal Shock Wave-Turbulent Boundary-Layer Interactions in the Presence of Streamwise Slots and Grooves," *Aeronautical Journal*, Vol. 106, No. 1063, 2002, pp. 493–500.

[12] Babinsky, H., "Active Control of Swept Shock Wave/Boundary Layer Interactions," *Drag Reduction by Shock and Boundary Layer Control: Results of the Project EUROSHOCK II Supported by the European Union, 1996-1999*, edited by E. Stanewsky, Springer–Verlag, Berlin, 2002, pp. 179–204.

[13] Krogmann, P., Stanewsky, E., and Thiede, P., "Effects of Suction on Shock/Boundary-Layer Interaction and Shock-Induced Separation," *Journal of Aircraft*, Vol. 22, No. 1, Jan. 1985, pp. 37–42.

[14] Stanewsky, E., "Aerodynamic Benefits of Adaptive Wing Technology," *Aerospace Science and Technology*, Vol. 4, No. 7, 2000, pp. 439–452.

[15] Delery, J., "Shock Phenomena in High Speed Aerodynamics: Still a Source of Major Concern," *Aeronautical Journal*, Vol. 103, No. 1019, Jan. 1999, pp. 19–34.

[16] Holden, H., and Babinsky, H., "Shock/Boundary Layer Interaction Control Using 3D Devices," AIAA Paper 03-0447, Jan. 2003.

[17] Inger, G., and Siebersma, T., "Computational Simulation of Vortex Generator Effects on Transonic Shock/Boundary-Layer Interaction," *Journal of Aircraft*, Vol. 26, No. 8, Aug. 1989, pp. 697–698.

[18] Holden, H. A., and Babinsky, H., "Separated Shock–Boundary-Layer Interaction Control Using Streamwise Slots," *Journal of Aircraft*, Vol. 42, No. 1, Jan.–Feb. 2005, pp. 166–171.